Customised Frequency Pre-Filtering in a Local Binary Pattern-Based Classification of Gastrointestinal Images

Sebastian Hegenbart[1], Stefan Maimone[1], Andreas Uhl[1], Andreas Vécsei[2], and Georg Wimmer[1]

[1] Department of Computer Sciences
University of Salzburg
Salzburg, Austria
[2] St. Anna Children's Hospital
Vienna, Austria
{gwimmmer,uhl}@cosy.sbg.ac.at

Abstract Local Binary Patterns (LBP) is a widely used approach for medical image analysis. Limitations of the LBP operator are its sensitivity to noise and its boundedness to first derivative information. These limitations are usually balanced by extensions of the classical LBP operator (e.g. the Local Ternary Pattern operator (LTP) or the Extended LBP (ELBP) operator). In this paper we present a generic framework that is able to overcome this limitations by frequency filtering the images as pre-processing stage to the classical LBP. The advantage of this approach is its easier adaption and optimization to different application scenarios and data sets as compared to other LBP variants. Experiments are carried out employing two endoscopic data sets, the first from the duodenum used for diagnosis of celiac disease, the second from the colon used for polyp malignity assessment. It turned out that high pass filtering combined with LBP outperforms classical LBP and most of its extensions, whereas low pass filtering effects the results only to a small extent.

Keywords: LBP, frequency filtering, medical image processing, endoscopy

1 Introduction

Computer-aided decision support systems relying on automated analysis of medical imagery receive increasing attention [1]. Among other techniques, feature extraction employing local binary patterns (LBP) is a popular approach which has been used for a wide variety of medical application domains, including colon polyp detection and classification [2], the diagnosis of celiac disease [3], and detection of gastric cancer [4] in classical flexible endoscopy, detection of ulcers [5], tumors [6], and blood [7] in capsule endoscopy images, and breast cancer diagnosis in microscopic specimens [8]. Even in traditional Chinese medicine (TCM) LBP have been applied, to distinguish between cold gastritis and heat gastritis in gastroscopic images [9].

The classical LBP operator has some limitations, as it is (i) sensitive to noise and (ii) can only reflect first derivative information since it is directly derived from the image intensity function. With respect to the first issue (i), the Local Ternary Pattern operator

(LTP) [10] has been introduced which uses a thresholding mechanism which implicitly improves the robustness against noise (a sort of implicit denoising is applied restricting the attention to low-frequency information), being especially important for many medical imaging modalities. Closely related are techniques applying the LBP operator to the approximation subband of a wavelet transform [3,11], since these data represent low-pass information as well which is hardly affected by noise. The second issue (ii) is tackled by introducing the Extended LBP (ELBP) [12] which applies a Gradient filter to the image before deriving LBP histograms. Closely related are techniques applying the LBP operator to detail subbands of a wavelet transform [13,14]. Some techniques attempt to deal with both issues concurrently, e.g. the Extended Local Ternary Pattern operator (ELTP [3]) integrates ELBP and LTP, and wavelet techniques including LBP information derived from approximation and details subbands (WTLBP), respectively [3,11].

All these proposed LBP extensions share the problem that their usage is somehow ad-hoc and that they are highly non-trivial to optimize to some specific setting, especially with respect to the extent of the frequency band the attention is restricted to. For example, classical wavelet subbands allow only an octave-based partitioning of frequency space and the usage of a spatial domain gradient operator does not offer siginificant adaptation potential at all.

These observations motivate the approach followed in this paper. As a generic framework we introduce a pre-filtering stage, in which we apply Fourier-based high-pass and low-pass filtering, respectively, before the LBP operator is applied to the filtered image material. In this manner, we have absolute control over the chosen cut-off frequency of the corresponding filter and are perfectly able to customize the frequency band the LBP operator is being applied to. We assess the effect of varying cut-off frequency and compare results of our generic framework to the abovementioned specialised LBP variants. Frequency filtering and the LBP operator are widely used applications for image processing, but the proposed combination of these two applications has not been proposed so far.

This paper is structured as follows. Section 2 explains the Fourier-domain filtering, as well as the LBP approach. Experimental results are shown in Section 3, where we provide comparatative classification results employing two endoscopic data sets, the first from the duodenum used for diagnosis of celiac disease, the second from the colon used for polyp malignity assessment. Section 4 concludes the paper and provides outlook to further refine the proposed approach.

2 Feature Extraction

2.1 Image filtering in the Frequency domain

In this section we shortly review image filtering to consider only their respective high frequency or low frequency information. Filtering is applied in the Fourier frequency domain.

A low pass filter in the frequency domain intuitively means zeroing all frequency components above a cut-off frequency and a high pass filter means zeroing all frequency

components beneath a cut-off frequency. We are normalizing the images frequencies so that they are between zero and one. That means for example that a low pass filter with cutoff frequency 1 is zeroing nothing and a low pass filter with cutoff frequency 0 is zeroing all frequencies. An ideal low pass filter (ILPF) is defined as follows:

$$h(u,v) = \begin{cases} 1 \text{ if } D(u,v) < D_0 \\ 0 \text{ otherwise} \end{cases} \tag{1}$$

where D_0 is the cut-off frequency and

$$D(u,v) = \frac{\sqrt{(u - M/2)^2 + (v - N/2)^2}}{\sqrt{(M/2)^2 + N/2)^2)}} \tag{2}$$

is the normalized distance of (u,v) ($u \in \{0,\ldots,M\},\ v \in \{0,\ldots,N\}$) to the center of the $(M+1) \times (N+1)$ image $I(u,v)$. The ideal high pass filter (IHPF) is defined conversly to the ILPF. Using ILPF and IHPF can result in unwanted ringing which is caused by the sharp transition from stop to pass band. To avoid this effect, one can smooth the transition between the stop and pass band. One example for a smoother filter is the Butterworth filter [15]. The Butterworth low pass (BLPF $h(u,v)$) and high pass filters (BHPF $g(u,v)$) are defined as follows:

$$h(u,v) = \tfrac{1}{1+(D(u,v)/D_0)^{2n}}, \qquad g(u,v) = \frac{1}{1 + (D_0/D(u,v))^{2n}}. \tag{3}$$

The higher the order n, the sharper the transition between the stop and pass band. For $n \to \infty$, the Butterworth LP (HP) filter converges toward the ILPF (IHPF).

In Figure 1 we see examples of filtered images. As cut-off frequencies we employ 0.06 for the high pass filters and 0.1 for the low pass filters.

Especially in case of the low pass filtered images we can see that the ILPF causes ringing while the BLPF avoids this effect. The high pass filtered images of the boy are looking quite different to the orginal image of the boy, while the high pass filtered endoscopic images of a healthy duodenum are looking quite similar to the original endoscopic image. That is because the endoscopic image does not contain visually significant low pass information in the filtered band.

After the filtering process, the frequency filtered image

$$I_h(u,v) = I(u,v)h(u,v) \text{ or } I_g(u,v) = I(u,v)g(u,v) \tag{4}$$

is transformed back to the spatial domain to apply the LBP operator to it like described in the following section.

2.2 Local Binary Patterns

The basic Local Binary Patterns (LBP) operator was introduced to the community by Ojala et al. [16]. The LBP operator considers each pixel in a neighborhood separately.

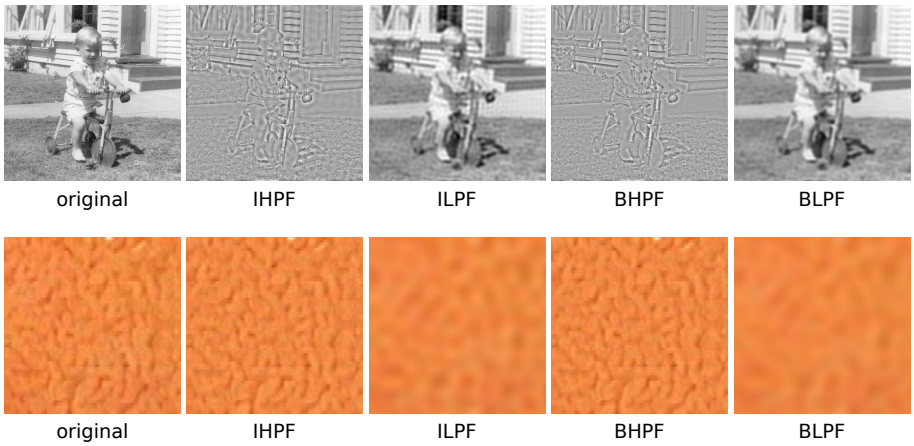

Figure 1. Examples of filtered images, a common image and an example from the celiac-dataset (see below).

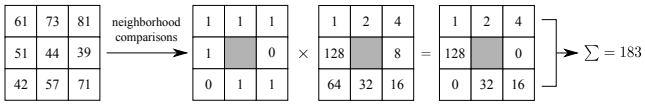

Figure 2. Demonstration of calculating the LBP operator

Hence the LBP could be considered a micro-texton. The operator is used to model a pixel neighborhood in terms of pixel intensity differences. This means that several common structures within a texture are represented by a binary label. The joint distributions of these labels are then used to characterize a texture. The LBP operator is defined as

$$LBP_{r,p}(x,y) = \sum_{k=0}^{p-1} 2^k \, s(I_k - I_c). \tag{5}$$

I_k is the value of neighbour number k and I_c is the value of the corresponding center pixel. The s function acts as sign function, mapping to 1 if the difference is smaller or equal to 0 and mapping to 0 else. In Figure 2 we can see an example for the calculation of the basic LBP operator for $p = 8$ and $r = 1$.

The LBP histogram of an image I is formally defined as

$$H_I(i) = \sum_{x,y} (LBP_{r,p}(x,y) = i) \qquad i = 0, \cdots, 2^p - 1. \tag{6}$$

The basic operator uses an eight-neighborhood ($p = 8$) with a 1-pixel radius ($r = 1$). To overcome this limitation, we use the notion of scale as discussed by Ojala et al. [17] by applying averaging filters to the image data before the operators are applied. Thus, information about neighboring pixels is implicitly encoded by the operator.

The appropriate filter sizes for a certain scale is calculated as described by Mäenpää [18]. We use three scale levels for the original LBP operator and all LBP variants (as mentioned in the Introduction) throughout this work. The histograms of the three scale levels are concatenated to form the feature vector of an image. For more details about the employed LBP variants see e.g. [3].

3 Experimental Study

3.1 Experimental Setup

Experiments are carried out using two medical image databases. The images of both databases are classified by the k-NN classifier using histogram intersection as metric. In case that experiments are applied to color images, LBP histograms are generated for each color channel and are finally concatenated.

The Celiac Disease Image Database: Celiac disease is a complex autoimmune disorder in genetically predisposed individuals of all age groups after introduction of gluten containing food. The celiac state of the duodenum is usually determined by visual inspection during the endoscopy session followed by a biopsy of suspicious areas. Images used are of size 128×128 and are divided into two classes according to their histologic state. The class denoted as "No-Celiac" represents a healthy duodenum with normal crypts and villi, whereas the class denoted as "Celiac" represents a duodenum with mild or marked atrophy of the villi or the villi are even entirely absent (see Figure 3). Especially feature extraction methods using high frequency information could be interesting to differentiate between the two classes, since images of patients with celiac disease have less or entirely no villi and so a lower amount of contrast compared to images of patients without celiac disease. That is one of the motivations to employ frequency filtering (especially high pass filtering) as preprocessing step to the feature extraction by means of LBP.

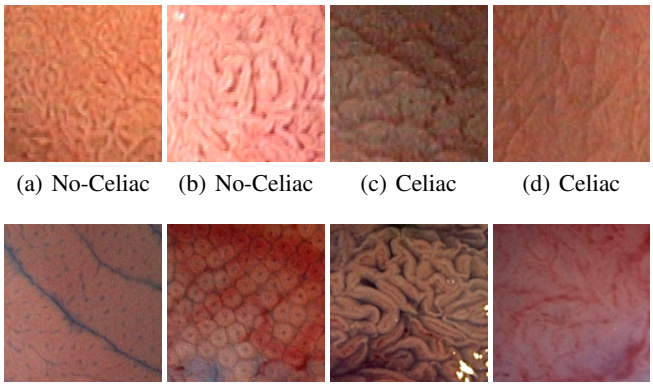

(a) No-Celiac (b) No-Celiac (c) Celiac (d) Celiac

(e) Normal (f) Normal (g) Abnormal (h) Abnormal

Figure 3. Images of the two classes from the duodenum ((a) – (d)) and from the colon ((e) – (h)).

The results of classifying the celiac disease database [19] are computed using an evaluation and a training set to avoid overfitting (Table 1 lists the number of image samples and patients per class). An image of the evaluation set is classified to the class, where the majority of its k nearest neighbors from the training set belong to. The k for the k-NN classifier, used to classify the test set, is between 1 and 25 and is optimized in the training set (the k with the highest accuracy using leave–one–out cross–validation (LOOCV) on the training set is used).

The Polyp Image Database: Polyps of the colon are a frequent finding and are usually divided into metaplastic, adenomatous and malignant [2]. A high magnifying colonoscope (magnification factor 150) is used to obtain images of the polyp's surface under indigo carmine staining, since images have to be as detailed as possible to uncover the fine surface structure of the mucosa as well as small lesions. The class denoted as "Normal" represents normal colon mucosa or hyperplastic polyps (non-neoplastic lesions), the class denoted as "Abnormal" represents neoplastic, adenomatous and carcinomatous structures (see Figure 3). As we notice from Figure 3, the pits of images from class Normal are regular and tightly distributed and are shaped similarly, in contrast to those of class Abnormal. Also for the polyp image database feature extraction methods using high frequency information could be helpful to distinguish the two classes, since the edge infornmation is important to detect the pits.

All images are of size 256×256, Table 1 lists the number of image samples and patients per class.

Table 1. Number of image samples per class of the two image databases (ground truth based on histology)

Celiac Disease						
	Training set			Evaluation set		
Class	No-Celiac	Celiac	Total	No-Celiac	Celiac	Total
Number of images	155	157	312	151	149	300
Number of patients	66	21	87	65	19	84

Polyp			
Class	Normal	Abnormal	Total
Number of images	199	518	716

In contrast to the celiac disease image database, the polyp image database [2] consists of images from too few patients (40) to devide them into an evaluation and a training set. To avoid overfitting as far as possible, we employ leave–one–patient–out cross–validation (LOPO) [19]. As k for the k-NN classifier, we use the one k between 1 and 25 with the highest overall classification rate (OCR).

3.2 Results

In Figure 4 we see four diagrams, which show how the cutoff frequency influences the results in terms of OCR accuracy, when frequency filtering is applied to the images of the two image databases followed by computing their LBP histograms. The red dotted line shows the result for the unfiltered images. The used Butterworth filters have order $n = 4$.

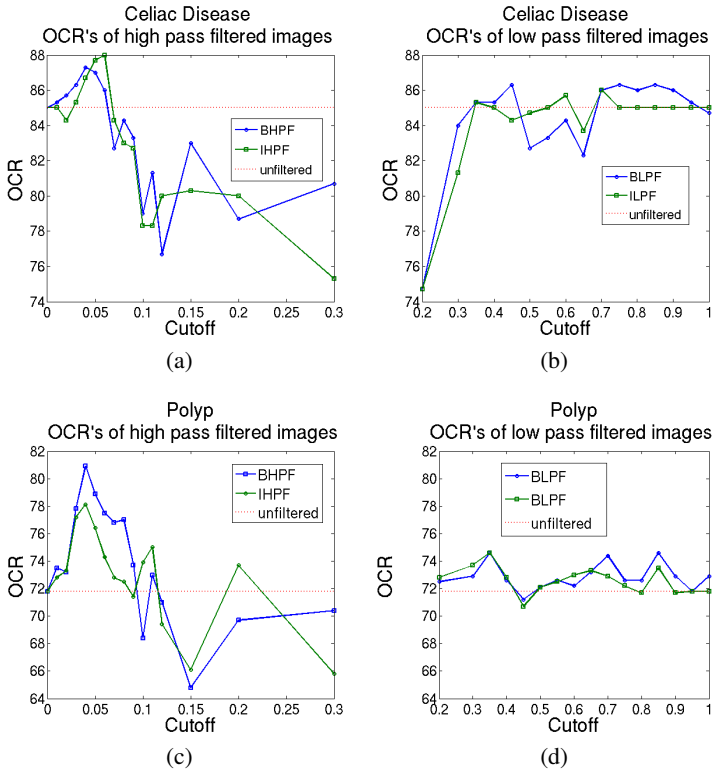

Figure 4. OCR accuracies of different cutoff frequencies for high pass and low pass filtered images of the two image databases.

As we can see, the results of the high pass filtered images are superior to those of unfiltered images for lower cutoff frequencies. For higher cutoff frequencies, results are worse than the results of the unfiltered image. The unfiltered images and the low pass filtered images have similar results, except for cutoff's ≤ 0.3 in case of the celiac disease image database.

In Table 2 we show comparatative results (i.e. LBP with pre-filtering vs. LBP variants) for the celiac disease database. Only the highest results across all tested cutoff frequencies are shown.

Table 2. Results of the LBP-variants applied to original and frequency filtered (LBP & ...) images of the celiac disease image database.

Colorspace	Grayscale			RGB		
Method	Sensitivity	Specificity	Accuracy	Sensitivity	Specificity	Accuracy
LBP & IHPF	91.3	84.8	88.0	89.3	79.5	84.3
LBP & BHPF	92.0	82.8	87.3	89.3	82.8	86.0
LBP & ILPF	89.9	82.1	86.0	85.2	80.8	83.0
LBP & BLPF	88.6	84.1	86.3	83.9	82.8	83.3
LBP	90.6	79.5	85.0	87.3	79.5	83.3
LTP	83.2	75.5	79.3	94.0	75.5	84.7
ELBP	94.0	74.2	84.0	93.3	81.5	87.3
ELTP	92.0	73.2	83.0	88.6	82.8	85.7
WTLBP	92.6	85.4	89.0	88.6	88.1	88.3

LBP applied to high pass filtered images works quite well compared to other LBP-based methods. Especially in case of the grayscale images, LBP applied to IHP filtered images works better than any other LBP-based method apart from WTLBP. Also for color images, high pass filtered image provide good results, but here color does not improve the grayscale results indicating a feature dimensionality problem.

Table 3. Results of the LBP-variants applied to the original and frequency filtered (LBP & ...) images of the polyp image database.

Colorspace	Grayscale			RGB		
Method	Sensitivity	Specificity	Accuracy	Sensitivity	Specificity	Accuracy
LBP & IHPF	96.9	28.8	78.1	96.0	43.3	84.1
LBP & BHPF	98.7	34.3	80.9	98.5	60.1	87.9
LBP & ILPF	96.0	18.7	74.6	96.1	59.1	85.9
LBP & BLPF	95.8	19.2	74.6	95.0	62.1	85.9
LBP	93.2	15.7	71.8	93.1	58.6	83.5
LTP	94.4	17.2	73.0	89.6	44.4	77.1
ELBP	92.5	37.9	77.4	96.1	56.7	85.2
ELTP	93.4	60.6	84.4	97.7	69.7	89.9
WTLBP	89.2	59.1	80.9	92.9	58.6	83.4

Table 3 shows the results for the polyp image database. Again, applying LBP to high pass filtered images provide better results than applying LBP to unfiltered or low pass filtered images. Especially the Butterworth variant is clearly superior in both the grayscale and RGB cases, respectively. Similar to the celiac disease dataset, the LBP & BHPF results are beaten only by LBP variants combining high pass and low pass filtering to some extent (i.e. ELTP, WTLBP).

Finally, we want to assess statistical significance of our results. The aim is to analyze if the images from the two databases are classified differently or similarly by the various LBP-based methods. We use the McNemar test [20], to test if two methods are significantly different for a given level of significance α by building test statistics from correctly and incorrectly classified images, respectively. Tests were carried out with a significance level of $\alpha = 0.01$. It turned out that there are no significant differences in case of the celiac disease database, contrary to the polyp database, where significant differences occur. The results for the polyp database (RGB color space) are displayed in Figure 5. We can observe, that LBP & BHPF is significant different to LBP, contrary to the methods LBP and LBP & IHPF. Also LBP & BHPF is significant different to LBP & IHPF, indicating that smoothing the transition between the stop and pass band (to avoiding ringing effects) has (a positive) impact on the classification results of the images when using the LBP operator as feature extraction method. The methods ELTP and LTP are significantly different to other methods, whereat ELTP works better and LTP works worse than the other methods.

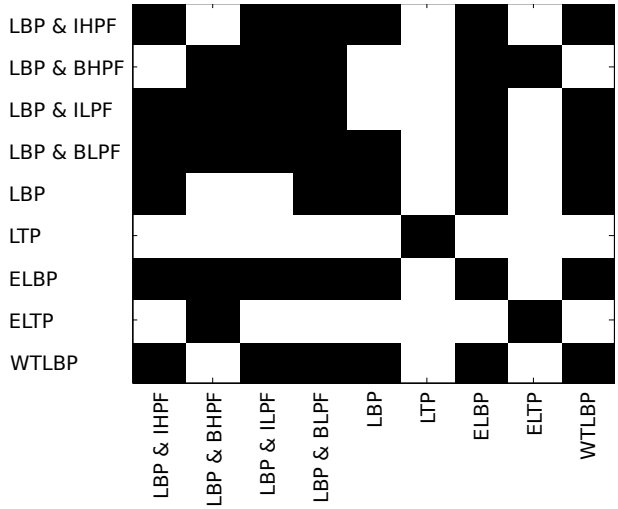

Figure 5. Results of the McNemar test for the polyp database. A white square in the i'th row and j'th column or in the j'th row and i'th column of a plot means that the i'th and the j'th method are significantly different with significance level $\alpha = 0.01$. If the square is black than there is no significant difference between the methods.

4 Conclusion

We have found that the generic framework of pre-filtering images before applying LBP feature extraction provides good results for our two endoscopic databases. Especially using high pass filters outperforms classical LBP and provides results competitive to

several LBP variants that have been proposed in literature. As we can see in [3], these LBP variants again outperform other classical medical image processing methods like Gabor Wavelets, Discrete Wavelet Transform or Dual-Tree Complex Wavelet Transform. So our proposed approach using high pass filters also works quite well compared to non-LBP based methods. An additional advantage of our approach is that it can be easily customised to a specific dataset by adjusting cut-off frequencies appropriately.

The reason we are focusing on high frequency information is, that high frequency information clearly points out the visible differences between healty and unhealthy mucosa on the two endoscopic data sets:

- In case of the celiac disease image database, images of patients with celiac disease have less or entirely no villi and so a lower amount of contrast compared to images of patients without celiac disease.
- In case of the polyp image database the edge information is important to detect the pits.

This is most likely the reason why our approach outperforms the classic LBP operator.

The proposed approach is only beaten by LBP variants which include both high pass and low pass filtering (WTLBP and ELTP) – based on this observation, we will consider in future work to use both high and low pass filtering in an adaptive manner where the optimal cut-off frequency is determined for both schemes (as indicated in Fig. 4) and the resulting LBP histograms are concatenated. Feature dimensionality can be controlled by applying feature subset selection techniques to bins of the resulting concatenated LBP histograms.

References

1. Liedlgruber, M., Uhl, A.: Computer-aided decision support systems for endoscopy in the gastrointestinal tract: A review. IEEE Reviews in Biomedical Engineering (2011) in press.
2. Häfner, M., Liedlgruber, M., Uhl, A., Vécsei, A., Wrba, F.: Color treatment in endoscopic image classification using multi-scale local color vector patterns. Medical Image Analysis **16**(1) (January 2012) 75–86
3. Vécsei, A., Amann, G., Hegenbart, S., Liedlgruber, M., Uhl, A.: Automated marsh-like classification of celiac disease in children using an optimized local texture operator. Computers in Biology and Medicine **41**(6) (June 2011) 313–325
4. Sousa, A., Dinis-Ribeiro, M., Areia, M., Coimbra, M.: Identifying cancer regions in vital-stained magnification endoscopy images using adapted color histograms. In: Proceedings of the 16th International Conference on Image Processing, 2009 (ICIP'09), Cairo, Egypt (November 2009) 681–684
5. Li, B., Meng, M.Q.: Texture analysis for ulcer detection in capsule endoscopy images. Image and Vision Computing **27**(9) (August 2009) 1336–1342
6. Li, B., Meng, M.Q.H.: Small bowel tumor detection for wireless capsule endoscopy images using textural features and support vector machine. In: Proceedings of the IEEE/RSJ International Conference on Intelligent Robots and Systems, St. Louis, USA (October 2009) 498–503
7. Li, B., Meng, M.Q.: Computer aided detection of bleeding regions for capsule endoscopy images. IEEE Transactions on Bio-Medical Engineering **56**(4) (April 2009) 1032–1039

8. Zhang, B.: Breast cancer diagnosis from biopsy images by serial fusion of random subspace ensembles. In: Biomedical Engineering and Informatics (BMEI), 2011 4th International Conference on. Volume 1. (October 2011) 180 –186
9. Xu, Z., Guo, H., Chen, W.: Gastritis cold or heat image research based on lbp. In: Computer, Mechatronics, Control and Electronic Engineering (CMCE), 2010 International Conference on. Volume 5. (August 2010) 331 –333
10. Tan, X., Triggs, B.: Enhanced local texture feature sets for face recognition under difficult lighting conditions. In: Analysis and Modelling of Faces and Gestures. Volume 4778 of LNCS., Springer (October 2007) 168–182
11. Wang, Y., chun Mu, Z., Zeng, H.: Block-based and multi-resolution methods for ear recognition using wavelet transform and uniform local binary patterns. (dec. 2008) 1 –4
12. Huang, X., Li, S., Wang, Y.: Shape localization based on statistical method using extended local binary pattern. In: Proceedings of the 3rd International Conference on Image and Graphics (ICIG'04), Hong Kong, China (2004) 1–4
13. Liu, X., You, X., Cheung, Y.: Texture image retrieval using non-separable wavelets and local binary patterns. In: International Conference on Computional Intelligence and Security, 2009. CIS '09, IEEE Computer Society (2009) 287–291
14. Su, Y., Tao, D., Li, X., Gao, X.: Texture representation in aam using gabor wavelet and local binary patterns. In: SMC'09: Proceedings of the 2009 IEEE international conference on Systems, Man and Cybernetics, Piscataway, NJ, USA, IEEE Press (2009) 3274–3279
15. Butterworth, S.: On the theory of filter amplifiers. Wireless Engineer **7** (1930) 536–541
16. Ojala, T., Pietikäinen, M., Harwood, D.: A comparative study of texture measures with classification based on feature distributions. Pattern Recognition **29**(1) (January 1996) 51–59
17. Ojala, T., Pietikäinen, M., Mäenpää, T.: Multiresolution Gray-Scale and rotation invariant texture classification with local binary patterns. IEEE Transactions on Pattern Analysis and Machine Intelligence **24**(7) (July 2002) 971–987
18. Mäenpää, T.: The local binary pattern approach to texture analysis - extensions and applications. PhD thesis, University of Oulu (2003)
19. Hegenbart, S., Uhl, A., Vécsei, A.: Systematic assessment of performance prediction techniques in medical image classification - a case study on celiac disease. In: Proceedings of the 22nd International Conference on Information Processing in Medical Imaging (IPMI'11), Monastery Irsee, Germany (July 2011) 498–508
20. McNemar, Q.: Note on the sampling error of the difference between correlated proportions of percentages. Psychometrika **12**(2) (June 1947) 153–157